

ROBOT VIBRATION CONTROL USING INERTIAL DAMPING FORCES

Soo Han Lee and Wayne J. Book
Georgia W. Woodruff School of Mechanical Engineering
Georgia Institute of Technology

ABSTRACT

This paper concerns the suppression of the vibration of a large flexible robot by inertial forces of a small robot which is located at the tip of the large robot. A controller for generating damping forces to a large robot is designed based on the two time scale model. The controller does not need to calculate the quasi-steady-state variables and is efficient in computation. Simulation results show the effectiveness of the inertial forces and the controller designed.

1. INTRODUCTION

The desire to improve manipulator arm performance has lead to designs with lighter arm structures. A light elastic structure responds to motion or disturbances with undesirable vibration, which must be either actively or passively damped before most manipulation tasks can be completed. A number of researchers have explored actively damping the vibrations with the joints of the flexible arm. [1,2,3] While this can be very effective, it requires high bandwidth servo control of the joints, with actuator bandwidth exceeding the vibrational frequencies to be damped.

This paper considers an alternative active control approach that is useful when additional degrees of freedom are available at the tip of the arm. In particular, we consider a small arm mounted on the end of a larger arm. This configuration is representative of proposed space manipulators and of bracing manipulators under study in several laboratories [4]. The small arm is used in this study to generate inertial forces on the large arm to cancel large arm vibrations. It is easier to provide high bandwidth actuators for a small arm than for a large arm. The large arm's function is to provide a base for the small arm, bringing the task into the small arm's work space. Highly accurate motion is not needed for the large arm, and providing it solely for active vibration control is a major compromise in cost and complexity. In fact, the large arm could be brought to position against a mechanical stop, or moved with a very simple on-off or open loop control.

This study involves simulation of a physical system for which later experiments are planned. The large arm, designated RALF (Robotic Arm Large and Flexible), is comprised of two ten foot long links and two hydraulically actuated joints. The second joint is actuated through a parallelogram mechanism by an actuator located near the base. Details on RALF, its modeling and experiments verifying its behavior are described in [5]. The small arm, designated SAM (Small Articulated Manipulator), is electrically powered and remains under construction at this time. It's three rotational joints give a spatial motion, but only two joints are considered here. As considered here SAM's first joint, which rotates about RALF's second link, has placed the four remaining joint axes of the system in a parallel direction and all motion considered is coplanar.

(NASA-CR-186808) ROBOT VIBRATION CONTROL
USING INERTIAL DAMPING FORCES (Georgia
Inst. of Tech.) R D CSCL 131

N90-25352

Unclass

65/37 0293322

2. DYNAMIC MODELING

Figure 1 shows a large flexible robot carrying a small rigid robot at its tip. There are four joint variables and infinite number of vibration variables. The most important variables to describe the dynamic system are four joint angles and one vibration variable for each flexible link [6]. However, in order to study the effectiveness of the inertial forces of a small robot, the angles of the large robot are assumed to be time invariant. By following [5], the dynamic equations of motion for the robot can be written in the following form.

$$M(\theta, q) \begin{bmatrix} \ddot{\theta} \\ \ddot{q} \end{bmatrix} + \begin{bmatrix} 0 \\ Kq \end{bmatrix} + \begin{bmatrix} N_{\theta}(\theta, \dot{\theta}, q, \dot{q}) \\ N_q(\theta, \dot{\theta}, q, \dot{q}) \end{bmatrix} = \begin{bmatrix} U \\ 0 \end{bmatrix} \quad (1)$$

where,

$M(\theta, q)$ is the inertia matrix,

$N(\theta, \dot{\theta}, q, \dot{q})$ includes nonlinear and gravity terms,

K is the stiffness matrix of the flexible robot,

θ is the vector of joint angles of small robot,

q is the vector of vibration amplitudes and

U is the actuator torque vector.

The singular perturbation technique is a useful method for simplifying the equations and reducing the order with modest reduction of model accuracy [7]. The flexible robot designed for industrial application, could have relatively high stiffness. In this case, the reduced order models comprised of fast and slow submodels can keep its original dynamic characteristics with negligible order of errors. The two reduced order submodels can be obtained by following [10,11] for the flexible robot. The equation (1) can be expressed as,

$$\begin{aligned} \ddot{\theta} &= -H_{12} Kq - H_{11} N_{\theta} - H_{12} N_q + H_{11} U \\ \ddot{q} &= -H_{22} Kq - H_{21} N_{\theta} - H_{22} N_q + H_{21} U \end{aligned} \quad (2)$$

where H is the inverse of mass matrix $M(\theta, q)$ and subscript i and j denote the corresponding submatrix.

To make the equation (2) a standard form as in [3], the inverse of the smallest spring constant k is selected as a perturbation parameter $\mu (=1/k)$. Then, the equation (2) can be written as following forms:

$$\ddot{\theta} = -H_{12} z - H_{11} N_{\theta} - H_{12} N_q + H_{11} U \quad (3a)$$

$$\mu z = -KH_{22} z - KH_{21} N_{\theta} - KH_{22} N_q + KH_{21} U \quad (3b)$$

where, $K = \mu K$, $z = Kq$, $H_{ij} = H_{ij}(\theta, \mu z)$, and $N_i = N(\theta, \dot{\theta}, \mu z, \dot{\mu z})$.

The equation for the slow submodel can be obtained by assuming $\mu=0$ which regards the flexible links as rigid. Substituting $\mu=0$ into the equation (3), we can obtain the following equations:

$$\ddot{\bar{z}} = \bar{H}_{22}^{-1} (-\bar{H}_{21}\ddot{\bar{\theta}} - \bar{H}_{22}\ddot{\bar{q}} + \bar{H}_{21}\ddot{\bar{U}}) \quad (4)$$

$$\ddot{\bar{\theta}} = -\bar{H}_{12}\ddot{\bar{z}} - \bar{H}_{11}\ddot{\bar{\theta}} - \bar{H}_{12}\ddot{\bar{q}} + \bar{H}_{11}\ddot{\bar{U}} \quad (5)$$

where bars are used to denote corresponding terms when $\mu = 0$ meaning the model dynamics are restricted to quasi-steady-state variables \bar{z} . \bar{U} is a slow control torque vector. The equation of slow submodel is obtained from equations (4) and (5) as

$$\ddot{\bar{\theta}} = \bar{M}_{11}^{-1} (-\bar{N}_{\theta} + \bar{U}) \quad (6)$$

The equation (6) is the same as that of a rigid robot.

In order to obtain the equation for the fast submodel, a scaled time $\tau = t/\sqrt{\mu}$ is introduced. Then, the equation (3b) can be rearranged as

$$\eta'' = -K\bar{H}_{22}\eta + K\bar{H}_{21}U_f \quad (7)$$

where $\eta = z - \bar{z}$ represents the deviation vector of the fast variables from the quasi-steady-state variables \bar{z} , $U_f = U - \bar{U}$ denotes fast control torque vector, and ' indicates differentiation with respect to τ . The equation (7) represents the fast submodel dynamics.

3. CONTROLLER DESIGN

To stabilize the two submodels, a composite control law is, generally, adopted [10] as

$$U = \bar{U}(\theta) + U_f(\eta)$$

The slow controller is used for controlling a rigid robot while the fast controller is used for forcing the fast deviation vector to approach to zero. For the slow submodel control, most of the well developed control laws for the rigid robot can be applied [9]. The nonlinear feedback controller is chosen as in [11].

$$\bar{U} = \bar{N}_{\theta} + \bar{M}_{11} (\ddot{\theta}_d - K_v(\dot{\theta} - \dot{\theta}_d) - K_p(\theta - \theta_d)) \quad (8)$$

where, subscript d denotes a desired value while K_v and K_p are gain matrices.

The gain matrices should be determined to keep the time scale separation between the controller bandwidth and lowest vibration frequency [12]. In simulation, the gains were chosen so the small rigid arm behaves as two decoupled joints, each with natural frequency of 6 rad/sec and damping ratio of one. This maintains a 4 to 1 separation from the lowest vibration frequency of 4 Hz.

The fast controller is usually designed using an optimal or eigenvalue assignment control law [9,10]. However, equation (7) has time-varying parameters. Hence, those control laws may not guarantee the stability of the controlled system. In addition, those controllers need the information about the quasi-

steady-state variables, \bar{z} . When the order of the dynamic equations is large as is the complete model in this case, the computation of \bar{z} takes up large amounts of processing time and may not be realistic for real time control. One of the main criteria for the fast controller design in this research is the capability of real time control. The equation (7) can be written in time t domain as

$$\dot{\eta} = -K \bar{H}_{22} \eta + K \bar{H}_{21} U_f \quad (9)$$

The equation (9) can be stabilized by applying the fast control torques as

$$K \bar{H}_{21} U_f = -K_{\eta v} \dot{\eta} \quad (10)$$

where, $K_{\eta v}$ denotes velocity gain matrix. The matrix \bar{H}_{21} is generally not invertible but will be in this case. However, the inverse of the matrix can be obtained using the pseudo-inverse technique. The signal, $\dot{\eta}$, used in the control can be written as

$$\dot{\eta} = \dot{z} - \dot{\bar{z}} = \dot{z} = K\dot{q} \quad (11)$$

Hence, the controller does not require information about \bar{z} and, therefore, is efficient in computation. It is generally known that adding a proportional control action to the controller can improve the performance. One would expect to be able to stiffen the system as well as increase its damping. However, there are physical limitations like the torque, joint travel, and bandwidth of actuators, or the time scale separation between controller bandwidth and the frequency of unmodeled dynamics. The controller satisfying equation (11) can relax the limitation. Thus, we design the fast controller as

$$U_f(q) = -\bar{H}_{21}^{-1} K_{\eta v} \dot{q} \quad (12a)$$

or

$$U_f(q) = -\bar{H}_{21}^T (\bar{H}_{21} \bar{H}_{21}^T)^{-1} K_{\eta v} \dot{q} \quad (12b)$$

where the equation (12b) is for the case when the matrix \bar{H}_{21} is not invertible. The composite controller is given as,

$$U = \bar{U}(\theta) + U_f(q)$$

In our simulation, the equation (12a) is used. The elements of the gain matrix are determined by considering the frequencies of vibration, 4 and 6 Hz, as $K_{\eta v11} = K_{\eta v22} = 20$ and $K_{\eta v12} = K_{\eta v21} = 0$. In order to compare the performance of the designed controller with full state feedback controller, the following modified nonlinear pole assignment control law is designed as

$$U_f(\eta) = (\bar{K} \bar{H}_{21})^{-1} (\bar{K} \bar{H}_{22} \eta - K_{fv} \eta' - K_{fp} \eta) \quad (13)$$

The elements of the gain matrix K_{fv} and K_{fp} are determined to yield two decoupled controllers each with a natural frequency of 60 rad/sec and a damping ratio of 0.5.

4. SIMULATION RESULTS

The control of the small manipulator SAM was simulated using the three control schemes described above. The joints of RALF, the large arm, were assumed to be locked as is representative of highly geared drives or stiff hydraulic actuators, at $\theta_1 = 60$ degrees and $\theta_2 = 120$ degrees. Results for an initial rate of deflection of RALF (Fig. 2, 3 and 4) with SAM in two nominal configurations and for a commanded motion of SAM (Fig. 5) are shown. The nominal configurations of SAM are $\theta_3 = 0$ and $\theta_4 = 60$ degrees (the design condition) and $\theta_3 = 10$, $\theta_4 = 50$ degrees (the off design condition).

First, the response of the system for no active attempt to respond to vibration of RALF is shown in Fig. 2. This is called the passive case. Only (8) is used to compute the control of SAM. As you see, the 6 rad/sec response of SAM's controller has superimposed on it the higher natural frequency of RALF at approximately 25 rad/sec (4 Hz). The vibration of the base due to RALF's dynamics are clearly visible in the motion of SAM's joints (Fig. 2) and in the displacement of the lower (Fig. 3) and upper (Not shown) link of RALF. Energy is slowly taken out of these vibrational modes by the motion of SAM as it is back driven by the disturbance. No damping is included in the model of RALF. The behavior is undesirable due to the long settling time of over 2 seconds.

A significant improvement in settling time of the vibration is achieved with active control of SAM in response to the vibrations of RALF as shown in Fig. 2, 3 and 4. The control is computed using both (8) and (12-a) and is referred to as deflection rate control. Under active feedback of the deflection rates, vibrations are damped in less than 1/2 the time required with passive control. A significant degradation is observed for the off design angles of SAM as shown in Fig. 4. The effectiveness of this control is sensitive to both the proper gains and the placement of SAM in a configuration to most effectively damp the vibrations. The large excursions of joint 4 in the off design condition (Fig. 4a) render the dashed case unacceptable. Joint torques (not shown) are also unacceptably high in this case.

An attempt to add deflection feedback to the deflection rate feedback is shown in Fig 2, labeled full state feedback. The control incorporates (8) and (13) using a pole placement scheme. The large excursion of SAM's joints point to difficulties predicted with this controller. The vibration of RALF is not damped as rapidly as with the deflection rate control as can be seen from Fig. 3a-b. Other methods of using full state feedback may prove more effective in future research.

When SAM is given a step command in desired angle, substantial excitation of RALF's vibration results. In Fig. 5 SAM's first joint (θ_3) is commanded to move from 0 to 30 degrees while θ_4 is commanded to move from 60 to 90 degrees. Both the passive and deflection rate control complete the move in 1 second, characteristic of the 6 rad/sec natural frequency of the slow control as shown in Fig. 5-a. The deflection rate fast control eliminates the deflection displacement almost simultaneously with completion of the commanded movement, however as seen in Fig. 5b and Fig. 5c. The passive control shows vibrations continuing well beyond 4 seconds.

5. CONCLUSIONS

Based on the results of simulation, the following conclusions are reached:

1. The inertia forces of the small robot are one of the effective ways to control the vibrations of the large flexible robot.
2. The dynamic equations of SAM and RALF are significantly simplified by singular perturbation technique and have proper time scale separation.
3. The designed damping control law shows good performance with much less computation than full state feedback control laws.
4. The nominal angles of SAM affect the performance of controller. The problems related to the angles will be addressed in a future paper.

Acknowledgements: This work was partially supported by NASA Grant NAG 1-623.

REFERENCES

1. Book, W. J., Maizza-Meto and Whitney, D. E., "Feedback Control of Two Beam, Two Joint Systems with Distributed Flexibility," ASME J. of Dynamics Systems, Measurement and Control, Vol. 97G, No. 4, December 1975.
2. Cannon, R. H. Jr., and Schmitz, E., "Initial Experiments on the End-Point Control of a Flexible One-Link Robot," Int. J. Robotics Research, Vol. 3, No. 3, 1984, pp. 62-75.
3. Truckenbrodt, A., "Truncation Problems in the Dynamics and Control of Flexible Mechanical Systems," Proc. 8th Triennial World Congress of IFAC, Vol. 7, 1982, pp. 1909-1914.
4. Book, W. J., Sanveraphunsiri, V. and Le, S., "Bracing Strategy for Robot Operation," Proc. of RoMan Sy '84: The 5th CISM-IFTOMM Symp. on Theory and Practice of Robots and Manipulators, Udine, Italy, June 1984, pp. 179-185.
5. Lee, J-W., Huggins, J. D., and Book, W. J., "Experimental Verification of a Flexible Manipulator," Proc. 1988 American Control Conference, Atlanta, GA, June 15-17, 1988, pp. 1021-1028.
6. Tsujisawa, T. and Book, W.J., "A Reduced Order Model Derivation for Light Weight Arms with a Parallel Mechanism," Proc., 1989 IS International Conference on Robotics and Automation, May 14-19, Scottsdale, AZ.
7. Kokotovic, P.V., "Applications of Singular Perturbation Technique to Control Problems," SIAM Review, Vol. 26, No. 4, 1984, pp. 501-550
8. Book, W.J. and Lee, Soohan, "Vibration Control of Large Flexible Manipulator by a Small Robotic Arm," Proceedings, 1989 American Control Conference, June 1989, Pittsburgh, PA
9. Siciliano, B. and Book, W.J., "A Singular Perturbation Approach to Lightweight Flexible Manipulators," International Journal of Robotics Research, Jan.. 1988.
10. Kokotovic, P., Khalil, H.K., and O'Reilly J. "Singular Perturbation Methods in Control: Analysis and Design," Academic Press, 1986
11. Luh, J.Y.S., Waker, M.W., and Paul, R.P.C., "Resolved- Acceleration Control of Mechanical Manipulators," IS Transactions on Automatic Control, Vol. AC-25, No. 3, June 1980, pp. 468-474
12. Khalil, H.K., "Output Feedback of Linear Two Time Scale System," Proceedings 1985 American Control Conference, New York, NY. pp. 1397-1400

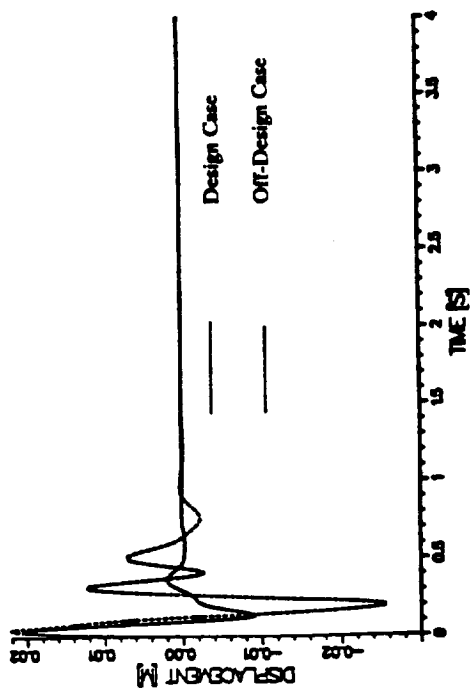


Figure 4b. Deflection Of Link 1 For Design And Off-Design Nominal Angles (θ_3 And θ_4). (RALF Has Initial Deflection Rates.)

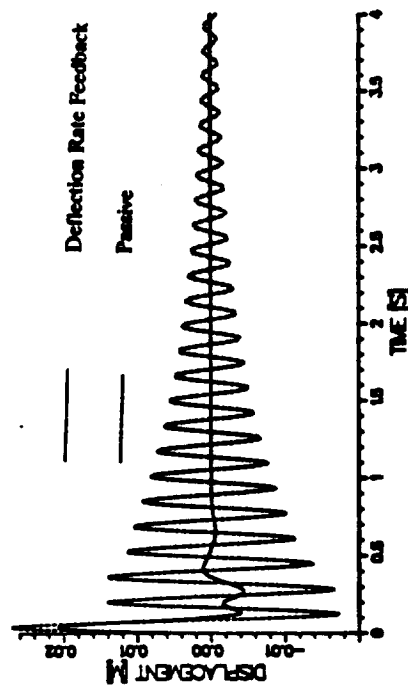


Figure 5b. Deflection Of RALF's Link 1 For The Commanded Motion In 5a.

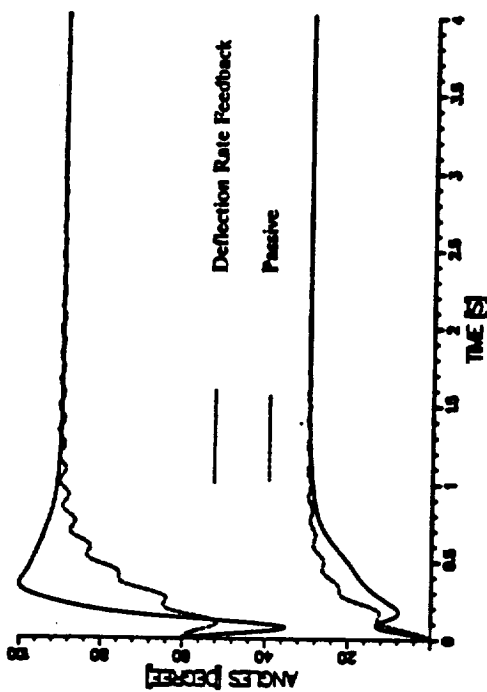


Figure 5a. Joint Response To A Step Command In Position Of θ_3 and θ_4 For Two Control Schemes. (RALF's Initial Conditions Are Zero.)

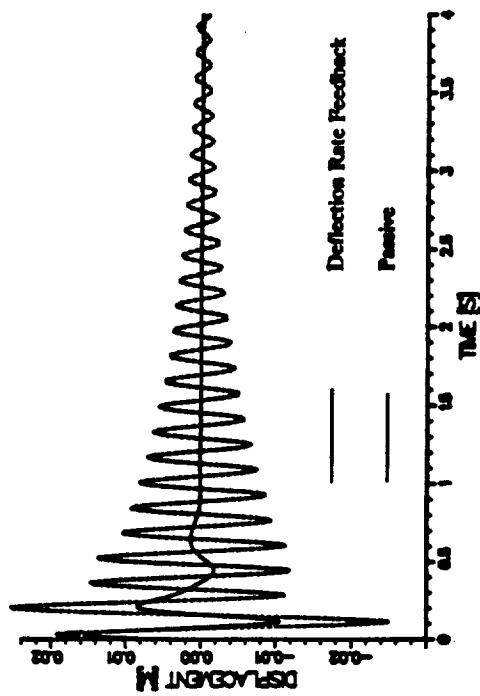


Figure 5c. Deflection Of RALF's Link 2 For The Commanded Motion In 5a.

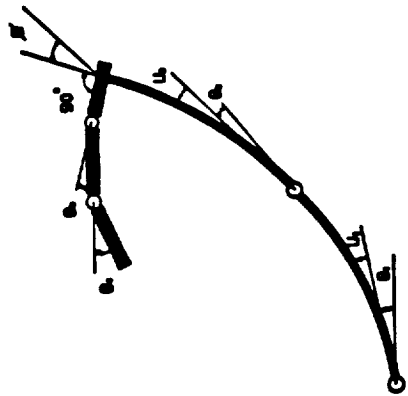


Figure 1. The System Of This Study: The Robotic Arm, Large And Flexible (RALF), Joints 1 And 2; Carrying The Small Articulated Manipulator (SAM), Joints 3 And 4.

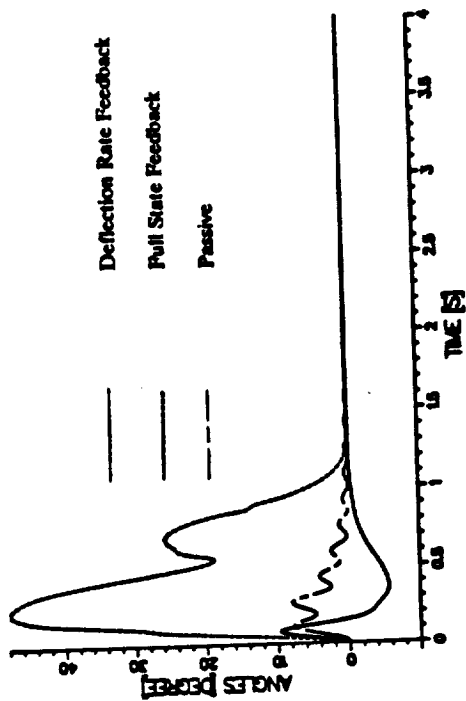


Figure 2. Motion Of SAM's First Joint (θ_3) For 3 Control Schemes. (RALF Has Initial Deflection Rates).

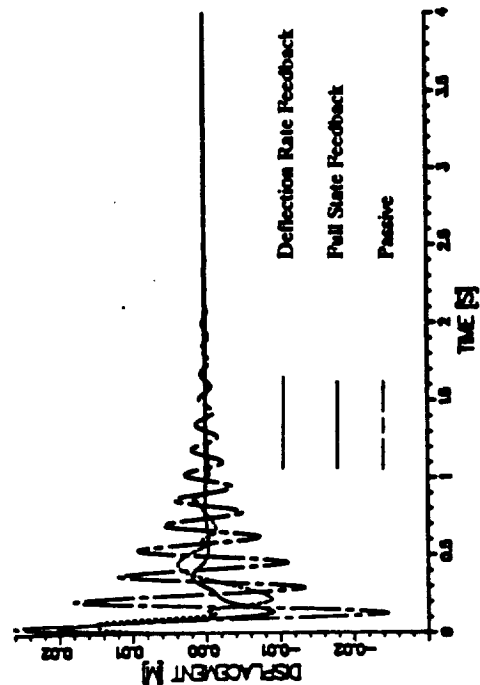


Figure 3. Deflection Of RALF's Link 1 For 3 Control Schemes. (RALF Has Initial Deflection Rates).

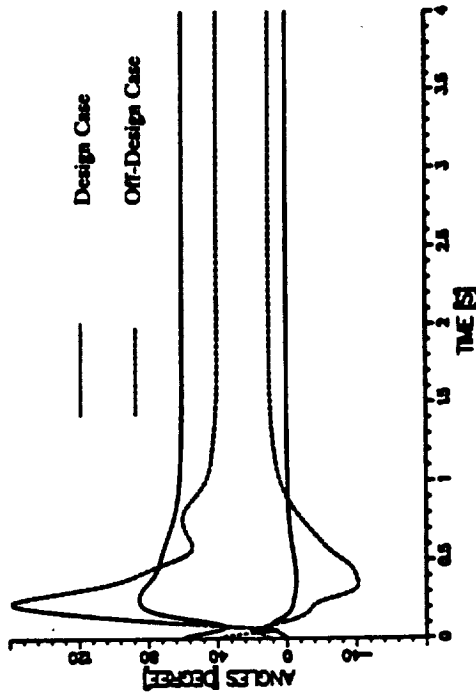


Figure 4a. Excursions Of SAM's Joints For Design And Off-Design Nominal Angles (θ_3 And θ_4). (RALF Has Initial Deflection Rates.)